

Influence of the phonon-mediated coupling on the properties of a single quantum-dot laserJia-pei Zhu,^{1,2} Hui Huang,¹ and Gao-xiang Li^{1,*}¹*Department of Physics, Huazhong Normal University, Wuhan 430079, China*²*Faculty of Science, Honghe University, Mengzi 661100, China*

(Received 12 December 2012; revised manuscript received 27 July 2013; published 19 August 2013)

We theoretically investigate the influence of the phonon-mediated coupling on the properties of the laser generated by a single red-detuned quantum dot (QD), where the QD is coherently driven and coupled to a microscopic cavity which can be engineered in a photonic band-gap (PBG) material. In the low-temperature limit, the phonon-mediated coupling is deleterious to the emission of photon into cavity field and the threshold behavior of the laser persists after the inclusion of the phonon-mediated processes. Without being engineered in the PBG material, if the damping rate κ of the cavity is close to but smaller than the phonon-mediated spontaneous emission rate γ of the dot, the photon statistics of the cavity field change from super-Poissonian to sub-Poissonian. The nonclassical effect can be achieved due to the phonon-mediated processes induced by the electron-phonon interaction and the off-resonant dot-cavity coupling. The nonclassical effect can be enhanced by the PBG material. When the effect of the thermal phonon is taken into account, the cavity field exhibits the super-Poissonian property. If κ is much smaller than γ , the phonon-mediated processes can lead to the increase (decrease) of the photons provided that the incoherent pumping rate is lower (higher) than the effective phonon-mediated threshold. But, if κ is close to or larger than γ , the emission of the photon may dominate the absorption process, strengthening the intensity of the cavity field.

DOI: [10.1103/PhysRevA.88.023835](https://doi.org/10.1103/PhysRevA.88.023835)

PACS number(s): 42.50.Ar, 42.50.Pq, 78.67.Hc, 42.70.Qs

I. INTRODUCTION

A single-emitter laser consisting of an atom in Rydberg [1] or lower electronic states [2], an ion [3], a superconducting qubit, or a quantum dot (QD) [4,5] interacting with a single-cavity mode is the fundamental model in the field of cavity quantum electrodynamics (CQED). Numerous interesting effects have been discovered in the behavior of single-emitter laser, such as squeezing [6], antibunching of photons [7], single and entangled photon sources [8], and observation of the vacuum-Rabi splitting in the spectrum [9]. It is a prerequisite for pumping rate exceeding that of relaxation when the conventional laser is generated, i.e., the pumping rate must be larger than the threshold of the lasing transition. The property of the thresholdless laser of a dressed atom is investigated [10], where a resonantly driven atom is strong coupled to a microcavity which is engineered in a photonic band-gap (PBG) material [11–14]. It is found that, under a thresholdless operation, mean photon number increases nonlinearly with the pumping rate, and this process is indicated by a sub-Poissonian statistics of the cavity field. Recently, a different analytical description is suggested to investigate the stationary behavior of a two-level emitter [15], which is shown to be a phase-averaged nonlinear coherent state (an eigenstate of a specific deformed annihilation operator) [16].

Every achievement with atoms becomes an objective for semiconductor because the semiconductor systems, e.g., a system based on semiconductor QDs embedded in photonic crystal nanocavities [17], allows for the design of scalable structure, hence possess unique advantages in terms of integration and scalability. The promising applications range from the studies of light-matter interaction, over ultralow-threshold lasers, to various applications in quantum information science

and integrated nanophotonic network. The ability of the photonic crystal microcavities to realize extremely small-microcavity mode volumes and very high-cavity Q factors endows it with a priority in realizing strong coupling [18]. Deterministic coupling a single QD to a photonic crystal cavity has been realized [19] and a thresholdless laser operating on a single QD is expected to be achieved [20]. Recently, the strong coupling of light and matter is reported to be realized with QDs in microcavities [21] and to be different from the paradigm of atoms in optical cavities.

One of the interesting developments in recent CQED experiments with QDs coupled to semiconductor microcavities is the observation of off-resonant dot-cavity coupling, in which excitations of one or more QDs embedded in a cavity also lead to a significant photon emission at cavity-field frequency. This fascinating phenomenon, initially reported by Hennessy *et al.* [22] and Press *et al.* [23], distinguishes the solid-state system from atomic CQED. Some theoretical [24,25] and experimental interests have been attracted to explore the physical mechanism behind such coupling as well as the possible applications. The power broadening of the QD linewidth and saturation of the cavity emission are observed [26,27] when measuring the spectroscopy of a resonantly driven QD which is coupled to an off-resonant cavity. The off-resonant coupling can be theoretically modeled by introducing a phenomenologically incoherent cavity pumping mechanism [28] to the coupled system. In contrast, an intuitive model for off-resonant coupling is proposed with inclusion of two additional incoherent decay terms into the dynamics of the system [25], referred to as phonon-mediated coupling. It appears that this model can properly describe the off-resonant dot-cavity coupling in a better way than the treatment of coupling between the QD and the cavity as a pure dephasing process, particularly in the case of large QD-cavity detuning [25]. On the other hand, the polaron transformation can eliminate the exciton-phonon coupling and introduces a

*gaox@phy.ccnu.edu.cn

modified dot-cavity coupling and a modified radiative-decay rate [29] and, consequently, is convenient for studying QD cavity-QED systems. A polaron master-equation method was proposed to describe the electron-phonon interaction (EPI) in the QD-cavity system [30,31]. Recently, the signatures of a coherently driven QD are demonstrated to be preserved after phonon-assisted scattering to an off-resonant cavity even for the presence of the incoherent scattering processes [32]. The phonon-mediated coupling between two QDs is also shown through an off-resonant photonic-crystal microcavity [33]. Besides, the strong coupling of a QD to a photonic molecule within a photonic crystal platform is studied as well as the observation of off-resonant cavity-cavity and QD-cavity interaction [34]. A solid-state CQED system with the bichromatic driving has also been investigated [35]. An endless pursuit for understanding the mechanism behind the off-resonant coupling and for its applications is going on. However, to the best of our knowledge, none of these works investigate the properties of the laser generated by a single QD which is off-resonant coupled with a cavity, and this is the task of this paper.

The purpose of this paper is to investigate the influence of the phonon-mediated coupling on the properties of the laser generated by a single strongly driven QD which is red detuned from and strongly coupled to a microcavity. It is found that, in a low-temperature limit, the phonon-mediated coupling plays a deleterious role in the mean photon number. The threshold behavior of the laser persists after the inclusion of the phonon-mediated processes. If the damping rate of the cavity κ is close to but smaller than the spontaneous emission rate γ of the dot, the photon statistics of the cavity field change from super-Poissonian to sub-Poissonian. The interesting nonclassical phenomenon can be achieved in the off-resonant dot-cavity system, without being engineered in a PBG material. This character should be attributed to the phonon-mediated processes induced by the EPI and the off-resonant dot-cavity coupling. When the effect of the thermal phonon is taken into account, the cavity field exhibits the super-Poissonian property. If the κ is much smaller than γ , the phonon-mediated processes can lead to the increase (decrease) of the photons in the cavity when the incoherent pumping rate is lower (higher) than the effective phonon-mediated threshold. But, if κ is close to or larger than γ , the emission process may dominate the absorption process, leading to the increase of the photon number in the cavity.

This paper is organized as follows. In Sec. II, we introduce the system and give the polaron master equation of the reduced density operator for the coupled dot-cavity system, in which the phonon-mediated coupling is explicitly included; then, we derive the equations for photon-number distribution function. Section III is devoted to the investigations of the influence of the phonon-mediated coupling on the properties of the laser. We first discuss the results in the limit of low temperature. Then, we explore the case when the effect of the thermal phonon is considered and give the reasonable explanations. Finally, we summarize our results in Sec. IV.

II. DESCRIPTION OF THE SYSTEM

The model for a single-emitter system strongly coupled to a microscopic cavity of frequency ω_c engineered inside

a PBG material was reported in previous literatures [10,12]. Our model consists of a single two-level QD and a high- Q microscopic cavity. The QD with ground state $|1\rangle$ and excited state $|2\rangle$ separated by transition frequency ω_a is driven by a coherent external laser field with frequency ω_L and Rabi frequency ε , and strongly coupled to the cavity which can be technically engineered within a photonic crystal. Aside from the coupling to the cavity, the QD is also allowed to interact with an acoustic-phonon reservoir. In the rotating frame with the frequency of ω_L , the Hamiltonian of the system can be written as (setting $\hbar = 1$ throughout the paper)

$$\hat{H} = \hat{H}_0 + \hat{H}_I, \quad (1)$$

in which the term

$$\begin{aligned} \hat{H}_0 = & \Delta_c a^\dagger a + \frac{\Delta_a}{2} \sigma_z + \varepsilon(\sigma_{12} + \sigma_{21}) \\ & + \sum_\lambda \Delta_\lambda a_\lambda^\dagger a_\lambda + \sum_p \omega_p b_p^\dagger b_p, \end{aligned} \quad (2)$$

representing the unperturbed Hamiltonians of the coherently driven QD under the rotating-wave approximation, the cavity, and the photonic crystal vacuum reservoir and the phonon reservoir. The operators a^\dagger (a), a_λ^\dagger (a_λ), and b_p^\dagger (b_p) are the creation (annihilation) operators for the microcavity mode, the photonic crystal vacuum reservoir, and the phonon reservoir, respectively. $\Delta_i = \omega_i - \omega_L$ ($i = a, c, \lambda$) describe the detunings between the transition frequency of the driven QD, the cavity-mode frequency, and the frequency of the crystal reservoir, from the driving frequency ω_L , respectively. $\sigma_{12} = \sigma_{21}^\dagger = |1\rangle\langle 2|$ is the lowering operator of the electron in the bare QD, and $\sigma_z = |2\rangle\langle 2| - |1\rangle\langle 1|$ corresponds to the population inversion operator.

In addition to the coupling with a single mode of a microcavity, the single QD is also allowed to interact with the photonic crystal vacuum reservoir and phonon reservoir. In practice, such a system can be realized by embedding a QD in a dielectric microcavity placed within a two-mode waveguide channel in a two-dimensional (2D) PBG microchip [12]. Under the rotating-wave approximation, the corresponding coupling can be given by the Hamiltonian within the electric dipole and rotating-wave approximations as

$$\begin{aligned} \hat{H}_I = & g_c(a^\dagger \sigma_{12} e^{i\Delta_c t} + a \sigma_{21} e^{-i\Delta_c t}) + \sum_p g_p \sigma_z (b_p + b_p^\dagger) \\ & + \sum_\lambda g_\lambda(\omega_\lambda) (a_\lambda^\dagger \sigma_{12} e^{i\Delta_\lambda t} + a_\lambda \sigma_{21} e^{-i\Delta_\lambda t}). \end{aligned} \quad (3)$$

The coefficients g_c , g_p , and $g_\lambda(\omega_\lambda)$ describe the coupling strength of the QD with the cavity mode, the phonon reservoir, and the vacuum modes of the photonic crystal, respectively. The information about the frequency dependence of the photonic crystal is stored in the coupling constant $g_\lambda(\omega_\lambda)$, which can be written as $g_\lambda(\omega_\lambda) = g_\lambda D(\omega_\lambda)$ with g_λ being a constant proportional to the dipole moment of the QD and $D(\omega_\lambda)$ corresponding to the transfer function of the reservoir. By appropriately engineering the system topology, at a certain frequency a large discontinuity in the local photon density of states (LDOS) can be produced, e.g., $|D(\omega_\lambda)|^2 = u(\omega_\lambda - \omega_b)$, where $u(\omega_\lambda - \omega_b)$ is the unit step function and ω_b refers to the photonic density-of-states band-edge frequency. The cavity

resonant frequency can be engineered to be within a PBG or low-LDOS region and near the LDOS discontinuity, such that the dot system which is strongly coupled to the cavity field also experiences this discontinuity which strongly influences the QD dynamics and results in new emission effects, i.e., $|D(\omega_\lambda)|^2 = 0$ for $\omega_\lambda > \omega_b$ and $|D(\omega_\lambda)|^2 = 1$ for $\omega_\lambda < \omega_b$. For a real band-gap material, the band edge is not exactly in the form of the step function but is rather in a form of a slope with width $\Delta\omega/\omega_b \approx 10^{-4}$ [11–14]. For example, for the case that the phonon-mediated spontaneous emission rate γ is of the order $10^{-6}\omega_b$, the cavity damping rate κ ranges from $10^{-9}\omega_b$ to $10^{-6}\omega_b$, and the Rabi frequency of the driving field is the order $10^{-3}\omega_b$, the unit-step-function approximation is reasonable [12]. In this regime, both the secular approximation and the rotating-wave approximation can be safely used in the system under consideration.

A. Polaron master equation in the dressed-states basis

For the convenience for studying this QD-cavity system, we transform the total system to the polaron frame [29–31] to eliminate the electron-phonon coupling and introduce a renormalized dot-cavity coupling strength. The polaron transformation of the QD-driven system can be written as $\tilde{H} = \exp(S)\hat{H}\exp(S)$ with

$$S = \sum_p \frac{g_p}{\omega_p} (b_p^\dagger - b_p) \sigma_z. \quad (4)$$

The transformed Hamiltonian of the system can be expressed as three parts

$$\tilde{H} = \tilde{H}_{\text{sys}} + \tilde{H}_{\text{bath}} + \tilde{H}_{\text{int}}, \quad (5)$$

where

$$\tilde{H}_{\text{sys}} = \frac{\Delta_a}{2} \sigma_z + \Delta_c a^\dagger a + \langle B \rangle \tilde{X}_g, \quad (6a)$$

$$\tilde{H}_{\text{bath}} = \sum_\lambda \Delta_\lambda a_\lambda^\dagger a_\lambda + \sum_p \omega_p b_p^\dagger b_p, \quad (6b)$$

$$\begin{aligned} \tilde{H}_{\text{int}} = & \sum_\lambda \langle B \rangle g_\lambda(\omega_\lambda) (a_\lambda^\dagger \sigma_{12} e^{i\Delta_\lambda t} + \text{H.c.}) \\ & + \tilde{X}_g \tilde{\Upsilon}_g + \tilde{X}_u \tilde{\Upsilon}_u \end{aligned} \quad (6c)$$

describe the Hamiltonian of a modified system (the QD plus the cavity), the baths (photonic vacuum and phonon reservoirs), and the interaction between the system and baths, respectively. In writing the expressions of Eq. (6), we have omitted the polaron shift $-\sum_p g_p^2/\omega_p$ which accounts for the renormalization of the resonant frequency of the QD because of phonon emission and reabsorption. In Eq. (6), we have defined the operators of the system as

$$\begin{aligned} \tilde{X}_g &= g_c (a^\dagger \sigma_{12} + a \sigma_{21}) + \varepsilon (\sigma_{12} + \sigma_{21}), \\ \tilde{X}_u &= i g_c (a^\dagger \sigma_{12} - a \sigma_{21}) + i \varepsilon (\sigma_{12} - \sigma_{21}), \end{aligned} \quad (7)$$

and the fluctuation operators of the phonon reservoir as

$$\begin{aligned} \tilde{\Upsilon}_g &= \frac{1}{2} (B_+ + B_- - 2\langle B \rangle), \\ \tilde{\Upsilon}_u &= \frac{1}{2i} (B_+ - B_-). \end{aligned} \quad (8)$$

Here, we have assumed that the phonon effect induced by the radiative decay processes has negligible contributions on our results thus treating B_\pm as $\langle B \rangle$ during the interaction of the QD with the photonic crystal vacuum reservoir. B_\pm is the coherent displacement operator of the phonon modes with the form

$$B_\pm = \exp \left[\pm \sum_p \frac{2g_p}{\omega_p} (b_p - b_p^\dagger) \right], \quad (9)$$

and $\langle B \rangle$ represents the thermally averaged values of the phonon displacement operators, which in general is of the form [31]

$$\begin{aligned} \langle B \rangle &= \exp \left[-\frac{1}{2} \int_0^\infty \frac{J(\omega)}{\omega^2} \coth \left(\frac{\omega}{2K_B T_p} \right) d\omega \right] \\ &= \exp \left[-\frac{1}{2} \sum_p \left(\frac{2g_p}{\omega_p} \right)^2 (2\bar{n}_p + 1) \right] \\ &= \langle B_+ \rangle = \langle B_- \rangle. \end{aligned} \quad (10)$$

$J(\omega)$ is the spectral function of the phonon reservoir. $\bar{n}_p \equiv \langle b_p^\dagger b_p \rangle = [\exp(\omega_p/K_B T_p) - 1]^{-1}$ is the mean phonon occupation number of frequency ω_p at a reservoir temperature T_p and K_B is the Boltzmann constant. Since $\hat{M} = \sum_p \frac{g_p}{\omega_p} b_p^\dagger$ and $\hat{N} = \sum_{p'} \frac{g_{p'}}{\omega_{p'}} b_{p'}$ satisfy the condition of $[\hat{M}, [\hat{M}, \hat{N}]] = [\hat{N}, [\hat{M}, \hat{N}]] = 0$, for simplicity, in this paper we apply the relation

$$e^{\alpha(\hat{M}+\hat{N})} = e^{\alpha\hat{M}} e^{\alpha\hat{N}} e^{-\alpha^2[\hat{M}, \hat{N}]/2} \quad (11)$$

and assume that the EPI is not strong such that the Taylor series expansion can be applied to approximately rewrite the displacement operators as $B_\pm \approx \langle B \rangle [1 \pm \sum_p \frac{2g_p}{\omega_p} (b_p - b_p^\dagger)]$. This treatment implies that we have neglected the processes involving multiphonon transitions.

Since the QD is strongly driven by a coherent field which can be viewed as a dressing field for the QD, we assume that the strength of the driven field is much stronger than that of the dot cavity ($\varepsilon \gg g_c$), and take the eigenstates defined by $\hat{H}_d = \Delta_a \sigma_z/2 + \langle B \rangle \varepsilon (\sigma_{12} + \sigma_{21})$ as the dressed states of the QD. The eigenstates of \hat{H}_d are obtained through the definition $\hat{H}_d |\alpha\rangle = \lambda_\alpha |\alpha\rangle$ with the form

$$|\tilde{1}\rangle = c|1\rangle - s|2\rangle, \quad |\tilde{2}\rangle = s|1\rangle + c|2\rangle, \quad (12)$$

where the parameters $c \equiv \cos \phi$ and $s \equiv \sin \phi$ with rotation angle $0 \leq \phi \leq \pi$ are defined as $c^2 = (1 + \frac{\Delta_a}{2\Omega})/2$ and $s^2 = (1 - \frac{\Delta_a}{2\Omega})/2$. $2\Omega = (4\langle B \rangle^2 \varepsilon^2 + \Delta_a^2)^{1/2}$ is the generalized Rabi frequency of the driving field. The operators $R_{ij} = |\tilde{i}\rangle \langle \tilde{j}|$ ($i, j = 1, 2$) correspond to the dressed-state transitions and the term $R_3^\dagger = |\tilde{2}\rangle \langle \tilde{2}| - |\tilde{1}\rangle \langle \tilde{1}|$ is the population inversion of the dressed QD. We point out here that despite the application of the external driving field, the lasing transition is pumped by a pure incoherent process. The coherent field appears here as a dressing field of the QD. Therefore, the process investigated in this paper is not the resonant scattering of coherent field. In this dressed-state basis, we transform the system into the interaction picture described by the unperturbed Hamiltonian

$$\tilde{H}_0 = \Delta_c a^\dagger a + \Omega R_3 + \sum_\lambda \Delta_\lambda a_\lambda^\dagger a_\lambda + \sum_p \omega_p b_p^\dagger b_p. \quad (13)$$

The interaction Hamiltonian of the system $\tilde{H}_{\text{int}}(t) = \exp(i\tilde{H}_0 t)\tilde{H}_{\text{int}}\exp(-i\tilde{H}_0 t)$ is correspondingly obtained as

$$\tilde{H}_{\text{int}}(t) = \hat{H}_I^\lambda(t) + \hat{H}_I^p(t), \quad (14a)$$

$$\begin{aligned} \hat{H}_I^\lambda(t) = & \sum_{\lambda} \langle B \rangle g_{\lambda}(\omega_{\lambda}) [c s a_{\lambda}^{\dagger} R_3 e^{i(\omega_{\lambda} - \omega_L)t} \\ & + c^2 a_{\lambda}^{\dagger} R_{12} e^{i(\omega_{\lambda} - \omega_L - 2\Omega)t} \\ & + s^2 a_{\lambda}^{\dagger} R_{21} e^{i(\omega_{\lambda} - \omega_L + 2\Omega)t} + \text{H.c.}], \end{aligned} \quad (14b)$$

$$\begin{aligned} \hat{H}_I^p(t) = & \sum_p \frac{2g_p}{\omega_p} \langle B \rangle [(g_c a^{\dagger} e^{i\Delta_c t} + \varepsilon)(c s R_3 + c^2 R_{12} e^{-i2\Omega t} \\ & - s^2 R_{21} e^{i2\Omega t}) - \text{H.c.}] (b_p e^{-i\omega_p t} - b_p^{\dagger} e^{i\omega_p t}). \end{aligned} \quad (14c)$$

In this paper, we only focus on the case of $\Delta_c = 2\Omega$, the coherently driven QD being red detuned from the cavity which is tuned to resonance with the high-frequency Rabi sideband. We assume that the central frequency ω_p of the phonon reservoir is nearly around 4Ω . In this case, we can employ the secular approximation to drop the terms oscillating at rapid frequencies such as $e^{\pm i\omega_p t}$, $e^{\pm i(\Delta_c \pm \omega_p)t}$, $e^{\pm i(2\Omega \pm \omega_p)t}$, $e^{\pm i(\Delta_c - 2\Omega \pm \omega_p)t}$, and $e^{\pm i(\Delta_c + 2\Omega + \omega_p)t}$. The interaction coupling (14c) reduces to

$$\hat{H}_I^p(t) = -\langle B \rangle \sum_p \frac{2g_p}{\omega_p} g_c s^2 (a R_{12} b_p^{\dagger} e^{i\Delta_p t} + \text{H.c.}), \quad (15)$$

where $\Delta_p = \omega_p - \Delta_c - 2\Omega$ represents the detuning of the phonon-mode frequency from the frequency of Δ_c plus the splitting frequency of the dressed states. The term $a R_{12} b_p^{\dagger} e^{i\Delta_p t}$ in Eq. (15) describes the process that the electron transits from the dressed state $|\tilde{2}, N-1\rangle$ to the upper dressed state $|\tilde{1}, N\rangle$ through the absorption of a cavity-mode photon and simultaneous emission of a phonon. Since the energy differences between the high-frequency transition of the dressed QD and the cavity frequency are compensated by the phonons with frequency $\omega_p \simeq 4\Omega$, the phonon-mediated processes discussed above and their counterparts occur resonantly.

In order to study the dynamics of the dot-cavity system, we assume that the couplings between the QD and the phonon and photonic crystal vacuum reservoirs are weak and the changes of the couplings in the reservoirs are negligible. Also, a fast time scale for the decay of the reservoir correlations is assumed such that the secular [36] and Born-Markov [37] approximations can be used. We apply the second-order perturbation theory to trace over the reservoir degrees of freedom and obtain the corresponding dissipative part of the master equation through the following equation:

$$\left(\frac{\partial \rho}{\partial t} \right)_{\lambda, p} = - \int_0^t dt' \text{Tr}_R \{ [\tilde{H}_{\text{int}}(t), [\tilde{H}_{\text{int}}(t'), \rho_T(t')]] \}, \quad (16)$$

where Tr_R denotes tracing over the photonic crystal vacuum reservoir and phonon reservoir variables. Under the Born-Markov approximation, the operator $\rho_T(t')$ in Eq. (16) will be replaced by $\rho(t) \otimes \rho_{\lambda}(0) \otimes \rho_p(0)$, where $\rho(t)$ is the reduced density operator for the dressed QD plus the cavity field and $\rho_p(0)$ and $\rho_{\lambda}(0)$ are the initial phonon and photonic crystal vacuum reservoir operators. After straightforward calculations, the master equation for reduced density operator of the coupled dot-cavity system, which can describe the

influence of the phonon-mediated off-resonant coupling on the dynamics of the dot-cavity system, has the form [12,38]

$$\frac{d\rho}{dt} = -i[\hat{H}_I', \rho] + \mathcal{L}_c \rho + \mathcal{L}_{\lambda} \rho + \mathcal{L}_p \rho. \quad (17)$$

In Eq. (17),

$$\hat{H}_I' = i g_1 (a^{\dagger} R_{12} - a R_{21}), \quad (18)$$

where $g_1 \equiv \langle B \rangle g_c c^2$ is the effective phonon-mediated coupling constant between the dressed dot and the off-resonant cavity. The first dissipative term $\mathcal{L}_c \rho = \kappa \mathcal{D}[a]$ in master equation (17) with the definition

$$\mathcal{D}[\mathcal{O}] = \frac{1}{2} (2\mathcal{O}\rho\mathcal{O}^{\dagger} - \mathcal{O}^{\dagger}\mathcal{O}\rho - \rho\mathcal{O}^{\dagger}\mathcal{O}) \quad (19)$$

is phenomenologically included, and describes the damping of the cavity mode into the crystal reservoir with decay rate κ . The second dissipative term $\mathcal{L}_{\lambda} \rho$ in master equation (17), originating from the interaction between the QD and the photonic crystal as described by Eq. (14b), is obtained as

$$\mathcal{L}_{\lambda} \rho = \gamma_0 \mathcal{D}[R_3] + \gamma_+ \mathcal{D}[R_{12}] + \gamma_- \mathcal{D}[R_{21}], \quad (20)$$

which is responsible for the damping among the dressed states of the dressed-QD system. Specifically, as shown in Fig. 1, the parameter $\gamma_0 = \gamma c^2 s^2 u(\omega_L - \omega_b)$ corresponds to the spontaneous emission rate with which the electron of the QD transits at central frequency of the dressed states. $\gamma = \tilde{\gamma} \langle B \rangle^2$ represents the phonon-mediated spontaneous emission rate and $\tilde{\gamma}$ is the spontaneous emission rate of the QD in free space. The coefficient $\gamma_- = \gamma s^4 u(\omega_- - \omega_b)$ corresponds to the phonon-mediated spontaneous decay rate of electron which occurs at frequency $\omega_- = \omega_L - 2\Omega$ from the lower dressed state $|\tilde{1}\rangle$ of one manifold with $N+1$ excitations to the upper dressed state $|\tilde{2}\rangle$ of the manifold below with N excitations [12,39], whereas the coefficient $\gamma_+ = \gamma c^4 u(\omega_+ - \omega_b)$ describes the decay rate of electron which occurs at frequency $\omega_+ = \omega_L + 2\Omega$ from the upper dressed state $|\tilde{2}\rangle$ of one manifold (with N excitations) to the lower dressed state $|\tilde{1}\rangle$ of the manifold below (with $N-1$ excitations), as depicted in Fig. 1.

Actually, the incoherent pumping process happens in the way from $|\tilde{1}\rangle$ with $N+1$ excitations to $|\tilde{2}\rangle$ with N excitations.

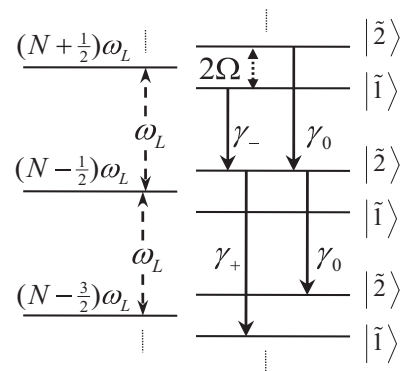


FIG. 1. Energy levels of the dressed-QD system with the transition rates to and out of the upper dressed state $|\tilde{2}\rangle$. The transition rate γ_+ corresponds to the phonon-mediated spontaneous emission rate at lasing frequency $\omega_L + 2\Omega$.

That is to say, the accumulation of the population in $|\tilde{2}\rangle$ with N excitations due to the incoherent pumping processes results from the annihilation of a photon from the driving field and simultaneous spontaneous emission of a photon with frequency $\omega_L - 2\Omega$. The lasing process occurs between $|\tilde{2}\rangle$ with N excitations and $|\tilde{1}\rangle$ with $N + 1$ excitations through the transition from $|\tilde{2}\rangle$ to $|\tilde{1}\rangle$, in which one cavity-mode photon with frequency $\omega_L + 2\Omega$ is created and one photon of the driving field is annihilated. As a result, the creation of a cavity-mode photon with frequency $\omega_L + 2\Omega$ is accompanied with the annihilation of two photons of the driving field and spontaneous emission of a photon with frequency $\omega_L - 2\Omega$. The laser can be generated only when the requirement $\gamma_- > \gamma_+, \gamma_0$ is satisfied because, in this case, these processes mentioned above occur repeatedly, leading to the continuous growth of the cavity photon number. Since the transitions between the dressed states occur at three frequencies ω_L , $\omega_L \pm 2\Omega$, and as referred previously that the cavity resonant frequency can be engineered to be within a PBG material, it is possible to eliminate spontaneous emission at the frequencies of ω_L and $\omega_L + 2\Omega$ by the strong driving with $\Omega \gg \gamma, \kappa, \gamma_p \bar{n}_p$, where γ_p and \bar{n}_p is the dissipation rate of the QD exciton and the mean number of the phonon bath. In this case, the thresholdless laser can be generated in the PBG material as discussed in Sec. III.

A lot of attention both from theoretical [25,31,32] and experimental [40,41] fields has focused on this interesting off-resonant dot-cavity system. The power broadening of the QD linewidth and saturation of the cavity emission are observed [26,27] when measuring the spectroscopy of a resonantly driven QD which is coupled to an off-resonant cavity. The signatures of a coherently driven QD are demonstrated to be preserved after phonon-assisted scattering to an off-resonant cavity even for the presence of the incoherent scattering processes [32]. The phonon-mediated coupling between two QDs is also shown through an off-resonant photonic-crystal microcavity [33]. The effect of the phonon-mediated coupling on the dynamics of the considered system is modeled by adding an additional incoherent decay term to the master equation [25]. Furthermore, a polaron master-equation method was proposed to describe the electron-phonon interaction (EPI) in the QD-cavity system [30,31]. More and more exciting achievements are reported. However, to the best of our knowledge, the investigation about the influence of the phonon-mediated processes arose due to the EPI and off-resonant dot-cavity coupling on the properties of the single-dot laser generated specially for the nonclassical field is yet vacant, and this is the main purpose of this paper. We find something interesting: (1) The threshold behavior of the laser persists after the inclusion of the phonon-mediated processes. (2) Without being engineered in the PBG material, the interesting nonclassical character can be generated due to the phonon-mediated processes that arose from the EPI and the dressed off-resonant coupling in the conventional dot-cavity system. (3) Nonclassical effect can be enhanced by the PBG material in the low-temperature limit. We believe that these could be useful for the relevant studies in such an off-resonant dot-cavity system.

We only focus on the case that the QD is red detuned from the cavity, i.e., $\Delta_c = 2\Omega$ and $\omega_p \simeq 4\Omega$. In this case, the

dissipative term $\mathcal{L}_p \rho$ induced by both the EPI and the off-resonant dot-cavity coupling is obtained after straightforward calculations following Eq. (16) as

$$\mathcal{L}_p \rho = s^4 \gamma_p (\bar{n}_p + 1) \mathcal{D}[a R_{12}] + s^4 \gamma_p \bar{n}_p \mathcal{D}[a^\dagger R_{21}], \quad (21)$$

where $\gamma_p = 2\pi g_c^2 \langle B \rangle^2 \sum_p (\frac{2g_p}{\omega_p})^2 \delta(\omega_p - 4\Omega)$ is the dissipation rate of the QD exciton states through the absorption of a photon and simultaneous emission of a phonon. $\bar{n}_p(\omega_p, T_p) = (e^{\omega_p/K_B T_p} - 1)^{-1}$ is the mean phonon occupation number at a bath temperature [31], where K_B is the Boltzmann constant. The term $\mathcal{D}[a R_{12}]$ describes the process in which the electron populated on the dressed state $|\tilde{2}\rangle$ transits to the state $|\tilde{1}\rangle$ with the absorption of a photon of the cavity field, while the term $\mathcal{D}[a^\dagger R_{21}]$ depicts the process with emission of a photon and simultaneous absorption of a phonon. Under the condition of $\Delta_c = 2\Omega$ and $\omega_p \simeq 4\Omega$, the processes described by both the terms $\mathcal{D}[a R_{21}]$ and $\mathcal{D}[a^\dagger R_{12}]$ nearly occur resonantly.

B. Equations for photon-number distribution function

To determine the characteristics of the coupled dot-cavity system and investigate the influence of the phonon-mediated coupling between the QD and the cavity, it is important to get the photon-number distribution function. In the following, we first derive the evolution equations of the density-matrix elements with respect to the dressed states of the QD, $\rho_{ij} = \langle \tilde{i} | \rho | \tilde{j} \rangle$. Considering the coherence of the dot-cavity system, we then introduce four combinations of these density-matrix elements and calculate the equations for them. Finally, we obtain the corresponding equations in the photon-number representation, from which the photon-number distribution function can be directly obtained.

For the case with $\Delta_c = 2\Omega$, the evolution equations of these density-matrix elements can be obtained by straightforward calculations from the master equation (17) as

$$\begin{aligned} \dot{\rho}_{11} &= g_1(a^\dagger \rho_{21} + \rho_{12}a) + \gamma_+ \rho_{22} - \gamma_- \rho_{11} + \kappa \mathcal{L}_c \rho_{11} \\ &\quad + \gamma_p (\bar{n}_p + 1) s^4 a \rho_{22} a^\dagger - \frac{\gamma_p \bar{n}_p}{2} s^4 (a a^\dagger \rho_{11} + \rho_{11} a a^\dagger), \\ \dot{\rho}_{22} &= -g_1(\rho_{21} a^\dagger + a \rho_{12}) - \gamma_+ \rho_{22} + \gamma_- \rho_{11} + \kappa \mathcal{L}_c \rho_{22} \\ &\quad - \frac{\gamma_p}{2} (\bar{n}_p + 1) s^4 (a^\dagger a \rho_{22} + \rho_{22} a^\dagger a) + \gamma_p \bar{n}_p s^4 a^\dagger \rho_{11} a, \\ \dot{\rho}_{12} &= g_1(a^\dagger \rho_{22} - \rho_{11} a^\dagger) - \frac{4\gamma_0 + \gamma_+ + \gamma_-}{2} \rho_{12} + \kappa \mathcal{L}_c \rho_{12} \\ &\quad - \frac{\gamma_p}{2} (\bar{n}_p + 1) s^4 \rho_{12} a^\dagger a - \frac{\gamma_p \bar{n}_p}{2} s^4 a a^\dagger \rho_{12}, \\ \dot{\rho}_{21} &= g_1(\rho_{22} a - a \rho_{11}) - \frac{4\gamma_0 + \gamma_+ + \gamma_-}{2} \rho_{21} + \kappa \mathcal{L}_c \rho_{21} \\ &\quad - \frac{\gamma_p}{2} (\bar{n}_p + 1) s^4 a^\dagger a \rho_{21} - \frac{\gamma_p \bar{n}_p}{2} s^4 \rho_{21} a a^\dagger, \end{aligned} \quad (22)$$

where $\rho_{11} = \langle \tilde{1} | \rho | \tilde{1} \rangle$ and $\rho_{22} = \langle \tilde{2} | \rho | \tilde{2} \rangle$ are the populations of the dressed states of the coupled dot-cavity system, $\text{Tr}_d(\rho) = \rho_{11} + \rho_{22}$ corresponds to the reduced density operator of the cavity field. Equation (22) has explicitly included the effect of the off-resonant coupling into the dynamics of the coupled system through the terms proportional to the dissipation rate

γ_p of the excited QD. In this paper, we use γ_p as well as \bar{n}_p to evaluate the influence of the phonon-mediated coupling.

In order to find the distribution function of the photon number of the cavity mode, we introduce four Hermitian combinations of the density-matrix elements:

$$\begin{aligned}\rho^{(1)} &= \rho_{22} + \rho_{11}, & \rho^{(2)} &= \rho_{22} - \rho_{11}, \\ \rho^{(3)} &= a^\dagger \rho_{21} + \rho_{12} a, & \rho^{(4)} &= \rho_{21} a^\dagger + a \rho_{12}.\end{aligned}\quad (23)$$

With these definitions, the evolution equations for these combinations $\rho^{(i)}$ can be obtained as Eqs. (A1) and (A2) (see the Appendix) via straightforward calculations for $\rho^{(i)}$ with the help of Eq. (22). After that, we expand these combined operators of the system in terms of the photon-number states $|n\rangle$ of the microcavity field. We find in the photon-number representation that the diagonal elements $P_n^{(i)} = \langle n | \rho^{(i)} | n \rangle$ satisfy the following equations of motion:

$$\begin{aligned}\dot{P}_n^{(1)} &= g_1 P_n^{(3)} - g_1 P_n^{(4)} + \kappa[(n+1)P_{n+1}^{(1)} - nP_n^{(1)}] + \frac{\gamma_p}{2}(\bar{n}_p + 1)s^4[(n+1)(P_{n+1}^{(1)} + P_{n+1}^{(2)}) - n(P_n^{(1)} + P_n^{(2)})] \\ &\quad + \frac{\gamma_p \bar{n}_p}{2}s^4[n(P_{n-1}^{(1)} - P_{n-1}^{(2)}) - (n+1)(P_n^{(1)} - P_n^{(2)})], \\ \dot{P}_n^{(2)} &= -g_1 P_n^{(3)} - g_1 P_n^{(4)} + \kappa[(n+1)P_{n+1}^{(2)} - nP_n^{(2)}] - \gamma_1 P_n^{(1)} - \gamma_{\text{pop}} P_n^{(2)} - \frac{\gamma_p}{2}(\bar{n}_p + 1)s^4[(n+1)(P_{n+1}^{(1)} + P_{n+1}^{(2)}) \\ &\quad + n(P_n^{(1)} + P_n^{(2)})] + \frac{\gamma_p \bar{n}_p}{2}s^4[n(P_{n-1}^{(1)} - P_{n-1}^{(2)}) + (n+1)(P_n^{(1)} - P_n^{(2)})], \\ \dot{P}_n^{(3)} &= g_1 n[P_{n-1}^{(1)} - P_n^{(1)} + P_{n-1}^{(2)} + P_n^{(2)}] + \kappa(n+1)P_{n+1}^{(3)} - \kappa P_n^{(4)} - \left[\gamma_{\text{coh}} + \frac{\kappa}{2}(2n-1) + \frac{\gamma_p}{2}s^4(2n\bar{n}_p + n-1) \right] P_n^{(3)}, \\ \dot{P}_n^{(4)} &= g_1(n+1)[P_n^{(1)} - P_{n+1}^{(1)} + P_n^{(2)} + P_{n+1}^{(2)}] + \kappa(n+1)P_{n+1}^{(4)} - \left[\gamma_{\text{coh}} + \frac{\kappa}{2}(2n+1) + \frac{\gamma_p}{2}s^4(2n\bar{n}_p + 2\bar{n}_p + n) \right] P_n^{(4)},\end{aligned}\quad (24)$$

where

$$\begin{aligned}\gamma_{\text{pop}} &= \gamma_+ + \gamma_-, & \gamma_1 &= \gamma_+ - \gamma_-, \\ \gamma_{\text{coh}} &= (4\gamma_0 + \gamma_+ + \gamma_-)/2.\end{aligned}\quad (25)$$

γ_{pop} and γ_{coh} are the resonance fluorescence decay rates for populations and coherence of the QD, respectively. In deriving Eq. (24), we have limited ourselves to the diagonal elements $P_n^{(i)} = \langle n | \rho^{(i)} | n \rangle$ since the equations can be decoupled for diagonal elements and the off-diagonal elements $\langle m | \rho^{(i)} | n \rangle (m \neq n)$ owing to the dependence of Eqs. (A1) and (A2) only on the bilinear combinations of the cavity-filled operators, i.e., the off-diagonal elements of these combinations are zero, which is in agreement with the result reported by Kilin *et al.* in Ref. [16]. The stationary behavior of the system is accessible if the photon-number distribution function $P^{(1)}$ is obtained. This can be achieved by solving Eq. (24) through the truncation of the photon number such that $P^{(1)}$ does not change when the number of the truncated states is increased.

The major difference of Eqs. (24) from that obtained in other models in a photonic crystal [10,12] is the appearance of those terms proportional to γ_p , which characterize the effect of the EPI between the QD and the cavity, which could lead to the absorption (emission) of a photon at cavity frequency and subsequent emission of a phonon when a electron transits from excited dressed state to the ground one of the QD which is red detuned from the cavity. The main purpose of this paper is to investigate the influence of the phonon-mediated processes on the properties of the laser.

III. RESULTS AND DISCUSSIONS

In this section, we will investigate the influence of the phonon-mediated processes that arose due to the EPI and

the off-resonant dot-cavity coupling on the properties of laser generated in the dot-cavity system which can be engineered within the PBG material. We evaluate the lasing properties of the cavity field using the steady-state mean photon number $\langle n \rangle$ and Mandel's Q parameter [42] which determines the statistics of the cavity field. $\langle n \rangle$ and Mandel's Q parameter are defined by the photon-number distribution function $P_n^{(1)}$ in the photon-number representation as

$$\langle n \rangle = \sum_{n=0}^{\infty} n P_n^{(1)}, \quad \langle n^2 \rangle = \sum_{n=0}^{\infty} n^2 P_n^{(1)}, \quad (26a)$$

$$Q = \frac{\langle (\Delta n)^2 \rangle - \langle n \rangle}{\langle n \rangle}. \quad (26b)$$

The Mandel's Q parameter is related to the Fano factor $F = \langle (\Delta n)^2 \rangle / \langle n \rangle$ via the relation $Q = F - 1$, which is usually used to identify the threshold behavior and nonclassical effect of the cavity field. Positive and negative values of Q indicate super- and sub-Poissonian statistics of the cavity field, respectively, and $Q = 0$ corresponds to a Poissonian case in which the state of the cavity field is coherent states.

In the following, we numerically solve the set of Eq. (24) to obtain the stationary value of the distribution function $P_n^{(1)}$ and the mean photon number and Mandel's Q parameter. We first discuss the influence of the phonon-mediated processes on the properties of laser in the low-temperature limit $\bar{n}_p = 0$. Then, we explore the case when taking the temperature of the thermal phonon into account and supply the reasonable explanations. The discontinuity function $u(\omega_- - \omega_b) = 1$ is set through the discussions and $u(\omega_+ - \omega_b) = 0$ and 1 represent the presence (shown with black lines) and absence (shown with red lines) of the PBG material, respectively. All parameters are scaled with

the phonon-mediated spontaneous emission rate γ in obtaining the numerical results.

A. Low-temperature limit $\bar{n}_p = 0$

As a simplification, we first consider the case of low-temperature limit, i.e., $\bar{n}_p = 0$, which indicates that we only care about the influence of the process described by the term $\mathcal{D}[aR_{12}]$ on the properties of laser and neglect the process described by the term $\mathcal{D}[a^\dagger R_{21}]$ in Eq. (21). In order to provide an overview of the different coupling schemes with respect to the damping rate κ of the cavity and the phonon-mediated spontaneous emission rate γ of the QD, we display our results from two aspects: (I) $\kappa < \gamma$, (II) $\kappa > \gamma$. Every case is discussed both for the presence and absence of the PBG material.

1. Case I: $\kappa < \gamma$

First, for the coupling scheme $\kappa < \gamma$, i.e., $\kappa = 10^{-3}\gamma$, we illustrate $\langle n \rangle$ and Mandel's Q parameter in Fig. 2 as a function of the incoherent pumping rate γ_- for different values of γ_p . Figure 2(a) shows a threshold behavior or a kink in the absence of the PBG material, and no threshold for the absence of the PBG material. The threshold behavior of the laser persists after the inclusion of the phonon-mediated processes.

The threshold of the laser can be understood as follows. As mentioned in Sec. II A, if the requirement $\gamma_- > \gamma_+$, γ_0

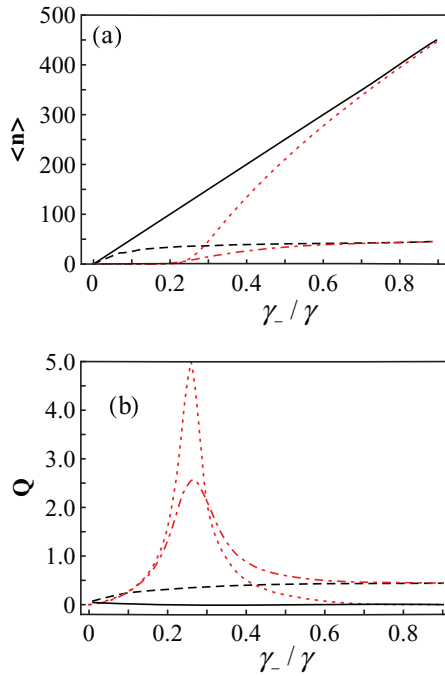


FIG. 2. (Color online) For $\bar{n}_p = 0$, the mean photon number $\langle n \rangle$ of the cavity field and Mandel's Q parameter are illustrated as a function of the incoherent pumping rate γ_- for different dissipation rate γ_p in the coupling scheme $\kappa = 10^{-3}\gamma$ with $g_1 = 10\gamma$. The discontinuity function $u(\omega_- - \omega_b)$ is set to be 1, and $u(\omega_+ - \omega_b) = 0$ and 1 represent the presence (black lines) and absence (red lines) of the PBG material, respectively. $\gamma_p = 0$, $u(\omega_+ - \omega_b) = 0$ for solid line, $\gamma_p = 0$, $u(\omega_+ - \omega_b) = 1$ for dotted line, $\gamma_p = 10^{-2}\gamma$, $u(\omega_+ - \omega_b) = 0$ for dashed line, $\gamma_p = 10^{-2}\gamma$, $u(\omega_+ - \omega_b) = 1$ for dotted-dashed line.

is satisfied, the lasing transition processes occur repeatedly, thus leading to the continuous growth of the cavity photon number. In the absence of PBG material, this requirement is equivalent to $s^4 > c^4$ or $\gamma_- > \gamma_-^0 = \gamma/4$. So, the threshold occurs when the pumping rate attains the value γ_-^0 , which corresponds to the population inversion between the dressed states of the lasing transition. The upper level $|\tilde{2}\rangle$ of the lasing transition is populated with the pumping rate γ_- simultaneously depopulated (relaxed) via the decay rate γ_+ , and reverse for the lower level $|\tilde{1}\rangle$ as indicated by $\mathcal{L}_2\rho$ in Eq. (20). Therefore, for a low pumping rate $\gamma_- < \gamma_-^0$, the pumping is weaker than the relaxation and no population inversion occurs. When the pumping is increased such that $\gamma_- > \gamma_-^0$, the pumping is stronger than the relaxation and the emission processes dominant over the absorption processes, thus leading to the generation of the laser [see Fig. 2(a)]. In the presence of the PBG material under consideration, the decay rate γ_+ as well as rate γ_0 of the state $|\tilde{2}\rangle$ with N excitations can be suppressed or eliminated so that the condition $\gamma_- > \gamma_+$ can be fulfilled even for a low pumping rate. The stimulated emission process dominates the absorption process of photons into the cavity field, thus leading to the generation of thresholdless laser. This threshold(less) behavior of laser, in agreement with what is described in Refs. [10,12], persists after the additional consideration of the electron-phonon coupling.

For $\Delta_a < 0$ ($\gamma_-/\gamma > \frac{1}{4}$), e.g., $\Delta_a = -5(B)\varepsilon$, $s^4 \simeq 0.9$, we also have $s^4 > c^4$. The population occupation in the dressed state $|\tilde{2}\rangle$ is dominant over that in $|\tilde{1}\rangle$ because the pumping rate γ_- is larger than the damping rate γ_+ . As mentioned in Sec. II A, the incoherent pumping process happens in the way from $|\tilde{1}\rangle$ with $N+1$ excitations to $|\tilde{2}\rangle$ with N excitations. The creation of a cavity-mode photon with frequency $\omega_L + 2\Omega$ is accompanied with the annihilation of two photons of the driving field and spontaneous emission of a photon with frequency $\omega_L - 2\Omega$. These processes mentioned above occur repeatedly, thus leading to the continuous growth of the cavity photon number as confirmed in Fig. 2(a).

On the other hand, it is also clearly shown in Fig. 2(a) that the mean photon number of the cavity field is decreased with the increasing of γ_p , which indicates that the inclusion of the phonon-mediated process induced by the EPI impedes the emission of photons into the cavity field, and leads to a reduction of the mean photon number. This effect is more obvious for a larger incoherent pumping rate. However, in the absence of PBG material, no obvious change of the threshold is found when the term $\mathcal{D}[aR_{12}]$ is considered, which implies that the phonon-mediated process described by $\mathcal{D}[aR_{12}]$, under the condition of $\bar{n}_p = 0$, does not affect the threshold of the laser. For the coupling scheme $\kappa = 10^{-3}\gamma$, when $\gamma_p = 0$, the Mandel's Q parameter has a sharp peak at $\gamma_-^0 = \frac{1}{4}\gamma$ [see Fig. 2(b)]. It is a clear indication of a threshold behavior. In the absence of the PBG material, with the increasing of γ_p , the phonon-mediated process reduces the Q parameter, but still being super-Poissonian. While the Q parameter is increased when the cavity is engineered within the PBG material, it is still around the Poissonian statistics as shown in Fig. 2(b).

Second, when the decay rate of the cavity is smaller than but close to the phonon-mediated spontaneous emission rate of

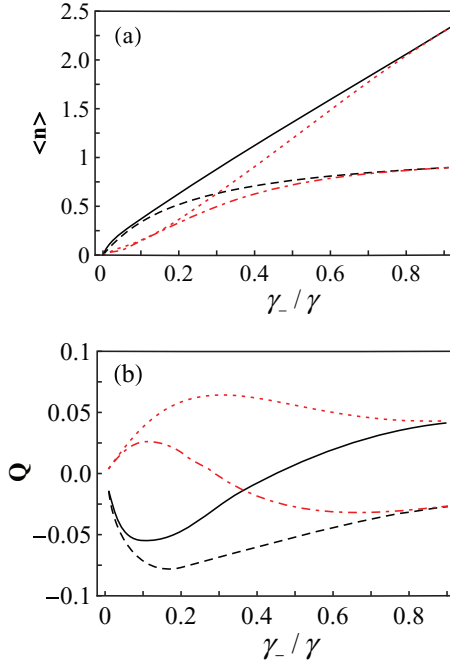


FIG. 3. (Color online) For $\bar{n}_p = 0$, the mean photon number $\langle n \rangle$ and Mandel's Q parameter of the cavity field are plotted as a function of γ_- for different values of γ_p in the coupling scheme $\kappa = 0.2\gamma$. $\gamma_p = 0$, $u(\omega_+ - \omega_b) = 0$ for solid line, $\gamma_p = 0$, $u(\omega_+ - \omega_b) = 1$ for dotted line, $\gamma_p = 0.8\gamma$, $u(\omega_+ - \omega_b) = 0$ for dashed line, $\gamma_p = 0.8\gamma$, $u(\omega_+ - \omega_b) = 1$ for dotted-dashed line. Other parameters are the same as in Fig. 2.

the QD, i.e., $\kappa = 0.2\gamma$, we plot $\langle n \rangle$ and Mandel's Q parameter in Fig. 3 as a function of γ_- for various values of γ_p . A reduction of the mean photon number of the cavity field is also induced by the phonon-mediated process. In the absence of the PBG material, due to the increasing of the ratio κ/γ_- , the kink becomes less visible. Another effect is that the mean photon number increases nonlinearly with the increase of the pumping rate, and this nonlinear effect is more prominent after inclusion of the phonon-mediated process regardless of the presence or absence of the PBG material, as shown in Fig. 3(a).

For a cavity with $\kappa = 0.2\gamma$ engineered in the PBG material, the nonlinear increase of the photon number is accompanied by a sub-Poissonian statistics of the cavity field. This sub-Poissonian character can be enhanced by the inclusion of the phonon-mediated process as shown with the black lines in Fig. 3(b). Here, we should stress that for a conventional cavity with $\kappa = 0.2\gamma$ and without being engineered in the PBG material $\gamma_+ = \gamma_-$, the photon statistics of the cavity field is Poissonian if the EPI is not considered, i.e. $\gamma_p = 0$, as shown by the dotted line in Fig. 3(b). However, by increasing γ_p , the photon statistics of the cavity field can be tuned to vary from Poissonian to sub-Poissonian in a wide range of pumping regimes, approaching a negative value of the Q parameter as confirmed by the dotted-dashed line in Fig. 3(b). This sub-Poissonian character should be attributed to the phonon-mediated processes induced by the EPI and the off-resonant dot-cavity coupling. It is different from the case $\gamma_p = 0$ where the Q parameter can not attain a negative value.

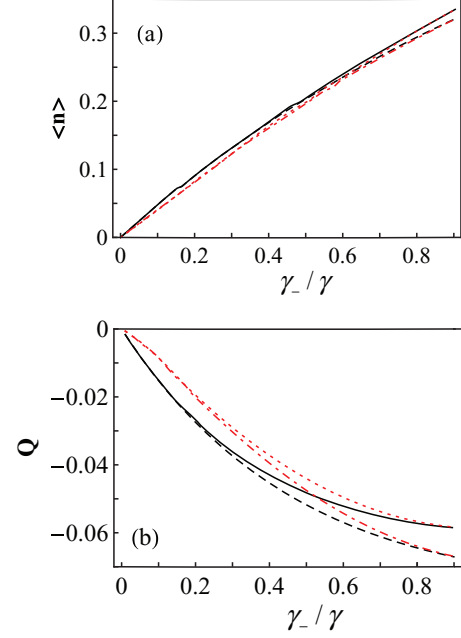


FIG. 4. (Color online) For $\bar{n}_p = 0$, $\langle n \rangle$ and Mandel's Q parameter are plotted as a function of γ_- for different values of γ_p in the coupling scheme $\kappa = 2\gamma$. $\gamma_p = 0$ and $u(\omega_+ - \omega_b) = 0$ for solid lines, $\gamma_p = 0$ and $u(\omega_+ - \omega_b) = 1$ for dotted lines, $\gamma_p = 0.5\gamma$ and $u(\omega_+ - \omega_b) = 0$ for dashed lines, $\gamma_p = 0.5\gamma$ and $u(\omega_+ - \omega_b) = 1$ for dotted-dashed lines. Other parameters are the same as in Fig. 2.

These discussions indicate that, in the case of low-temperature limit $\bar{n}_p = 0$, the interesting nonclassical character can be generated in a conventional off-resonant dot-cavity system, without being engineered in a PBG material.

2. Case II: $\kappa > \gamma$

Figure 4 illustrates $\langle n \rangle$ and Mandel's Q parameter as a function of γ_- for γ_p being 0 and 0.5γ in the coupling scheme $\kappa = 2\gamma$. In this scheme, the photon number is small, therefore the contributive lasing transitions are limited. So, the effect of the phonons is deleterious to, but has little influence on, the photon number as shown in Fig. 4(a). When $\kappa = 2\gamma$, the Mandel's Q parameter is negative both for the presence and absence of the PBG material. The inclusion of the phonon-mediated processes as well as the role of the PBG material can reduce the value of Q and enhance the nonclassical effect of the photon field [see Fig. 4(b)].

These numerical discussions about the influence of the phonon-mediated process can be explained as follows. The process, in which the relaxation of the excited QD occurs through the emission of a photon and simultaneous absorption of a phonon as described by the term $\mathcal{D}[a^\dagger R_{21}]$ in Eq. (21), is neglected through the low-temperature limit $\bar{n}_p = 0$. Only the process described by the term $\mathcal{D}[a R_{12}]$ in Eq. (21) is allowed to occur, which will lead to the absorption of photon at the cavity frequency and emission of a phonon due to the EPI. Therefore, when the phonon-mediated dot-cavity coupling is taken into account, it is not a surprise that a reduction of the mean photon number of the cavity field is induced as indicated especially from Figs. 2(a) and 3(a).

As discussed above, under the condition of $\bar{n}_p = 0$, the phonon-mediated processes induced by the EPI and the off-resonant dot-cavity coupling could lead to a reduction of the photon number. The threshold behavior is preserved, but the value of Mandel's Q parameter is reduced. It is worth pointing out that, for a cavity with $\kappa = 0.2\gamma$ and without being engineered in a PBG material, the photon statistics of the cavity field can be changed from Poissonian to sub-Poissonian by increasing γ_p . The interesting nonclassical effect can be achieved for the off-resonant dot-cavity system, without being engineered in a PBG material. This character should be attributed to the phonon-mediated processes induced by the EPI and the off-resonant dot-cavity coupling. In the following section, we take the effect of the thermal phonon into account, i.e., $\bar{n}_p \neq 0$, to investigate the property of the laser.

B. Role of the temperature of the phonon bath $\bar{n}_p \neq 0$

The phonon number \bar{n}_p , characterizing the temperature of the phonon reservoir, in experimental systems is generally not negligible. Taking $\bar{n}_p = 5$ as an example, we illustrate the mean photon number $\langle n \rangle$ of the cavity field and Mandel's Q parameter as a function of the incoherent pumping rate γ_- for different damping rate γ_p in Figs. 5–7. For the parameters mentioned before, with ω_b being the order of 10^{14} Hz and $\Omega \sim 10^{11}$ Hz (corresponding to 0.41 meV), the central frequency ω_p of the phonon bath approximating 4×10^{11} Hz, an estimated temperature of the order 10 K is

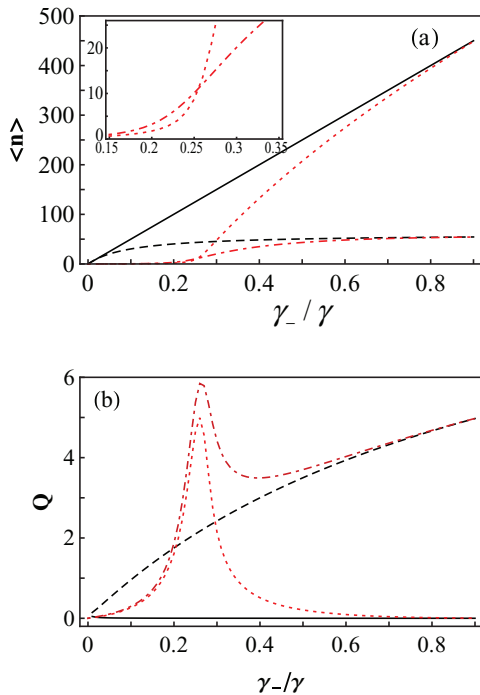


FIG. 5. (Color online) Same as in Fig. 2 except $\bar{n}_p = 5$. (a) $\gamma_p = 0$ and $u(\omega_+ - \omega_b) = 0$ for solid lines, $\gamma_p = 0$ and $u(\omega_+ - \omega_b) = 1$ for dotted lines, $\gamma_p = 0.01\gamma$ and $u(\omega_+ - \omega_b) = 0$ for dashed lines, $\gamma_p = 0.01\gamma$ and $u(\omega_+ - \omega_b) = 1$ for dotted-dashed lines. (b) $\gamma_p = 0$ and $u(\omega_+ - \omega_b) = 0$ for solid lines, $\gamma_p = 0$ and $u(\omega_+ - \omega_b) = 1$ for dotted lines, $\gamma_p = 10^{-3}\gamma$ and $u(\omega_+ - \omega_b) = 0$ for dashed lines, $\gamma_p = 10^{-3}\gamma$ and $u(\omega_+ - \omega_b) = 1$ for dotted-dashed lines. The inset of (a) shows an enlarged view of $\langle n \rangle$.

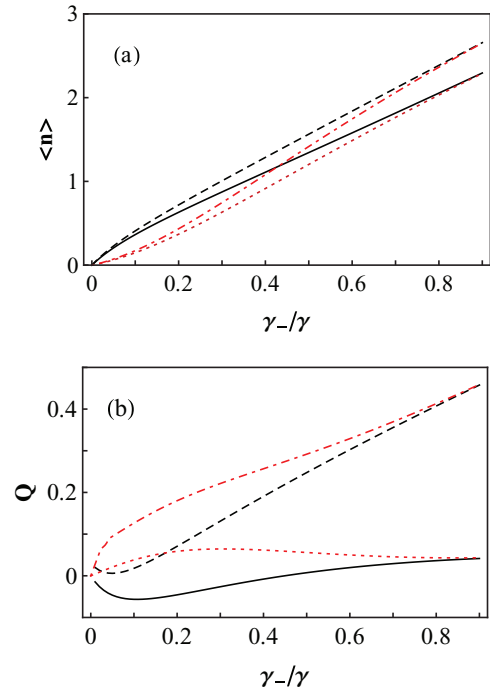


FIG. 6. (Color online) Same as in Fig. 3 except $\bar{n}_p = 5$. $\gamma_p = 0$ and $u(\omega_+ - \omega_b) = 0$ for solid lines, $\gamma_p = 0$ and $u(\omega_+ - \omega_b) = 1$ for dotted lines, $\gamma_p = 0.01\gamma$ and $u(\omega_+ - \omega_b) = 0$ for dashed lines, $\gamma_p = 0.01\gamma$ and $u(\omega_+ - \omega_b) = 1$ for dotted-dashed lines.

obtained. We find that the influence of the phonon-mediated processes on $\langle n \rangle$ and Mandel's Q parameter is different from the case of $\bar{n}_p = 0$. The behaviors of $\langle n \rangle$ in different schemes are discussed first, then the corresponding behaviors of the Mandel's Q parameter.

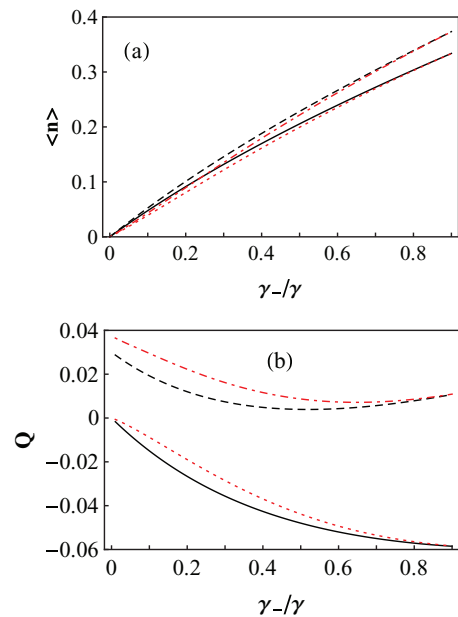


FIG. 7. (Color online) Same as in Fig. 4 except $\bar{n}_p = 5$. $\gamma_p = 0$ and $u(\omega_+ - \omega_b) = 0$ for solid lines, $\gamma_p = 0$ and $u(\omega_+ - \omega_b) = 1$ for dotted lines, $\gamma_p = 0.01\gamma$ and $u(\omega_+ - \omega_b) = 0$ for dashed lines, $\gamma_p = 0.01\gamma$ and $u(\omega_+ - \omega_b) = 1$ for dotted-dashed lines.

For a cavity whose damping rate is much smaller than the spontaneous emission rate of the QD, i.e., $\kappa = 10^{-3}\gamma$, it seems from Fig. 5(a) that the mean photon number of the cavity field is obviously reduced due to the phonon-mediated processes, and this reduction is pronounced for a large value of the pumping rate. This is similar to the case of the low-temperature limit. However, for the cavity without being engineered in the PBG material, it is shown in the inset of Fig. 5(a) that the plots for the photon number $\langle n \rangle$ with different values of γ_p converge at $\gamma_-^0 \simeq 0.27\gamma$, which plays the role of a new effective phonon-mediated threshold. This fact indicates that the phonon-mediated processes reduce the mean photon number of the cavity field only when $\gamma_- > \gamma_-^0$; if $\gamma_- < \gamma_-^0$, the effect of the inclusion of the phonon-mediated processes is to increase, rather than reduce, the mean photon number of the cavity field. This implies that, for a good cavity, when the incoherent pumping γ_- is smaller than the new effective phonon-mediated threshold γ_-^0 , the phonon-mediated processes may stimulate extra emission of photon into the cavity field, leading to an increase of the photon number.

For $\bar{n}_p = 5$, if the damping rate of the cavity is close to or larger than the spontaneous emission rate of the QD, i.e., $\kappa = 0.2\gamma$ and 2γ , the mean photon number of the cavity field is increased rather than decreased with the increase of γ_p regardless of the presence or absence of the PBG material as shown in Figs. 6(a) and 7(a), which is surprisingly different from the ideal case with zero temperature $\bar{n}_p = 0$, where the inclusion of the phonon-mediated processes is deleterious to the emission of a photon into the cavity field. In this case, the intensity of the cavity photon could be strengthened by phonon-mediated processes that arose from the EPI and the off-resonant dot-cavity coupling. The increase of $\langle n \rangle$ with γ_- is also nonlinear.

In fact, for $\bar{n}_p \neq 0$, two types of processes described by Eq. (21) are involved during the relaxation of the excited QD. As discussed before, the term $\mathcal{D}[aR_{12}]$ describes the process in which the electron populated on the excited dressed state $|\tilde{2}\rangle$ transits to the state $|\tilde{1}\rangle$ with the absorption of a photon and simultaneous generation of a phonon, while the term $\mathcal{D}[a^\dagger R_{21}]$ depicts the process with emission of a photon and simultaneous absorption of a phonon. In this case, whether the effect of the presence of the phonon-mediated coupling is to increase or decrease the mean photon number of the cavity field depends on the strength of these two types of competitive processes. For the case of $\kappa = 10^{-3}\gamma$, the electronic degrees of the QD are in the steady state. It is reasonable to decouple the QD from the cavity, thus the strength of the absorption and emission processes of photons can be approximated as $s^4\gamma_p(\bar{n}_p + 1)\rho_{22}$ and $s^4\gamma_p\bar{n}_p\rho_{11}$, respectively. The quantity $W = \gamma_p s^4[(\bar{n}_p + 1)\rho_{22} - \bar{n}_p\rho_{11}]$ is illustrated as a function of γ_- in Fig. 8. It is clearly indicated from Fig. 8 that the emission processes of photons dominate the absorption processes when the incoherent pumping rate γ_- is below the new effective phonon-mediated threshold γ_-^0 and the inverse for $\gamma_- > \gamma_-^0$. Therefore, the photon number is increased when $\gamma_- < \gamma_-^0$, and reduced when $\gamma_- > \gamma_-^0$ as confirmed in Fig. 5(a). For the case of $\kappa = 0.2\gamma$ considered in Fig. 6 and $\kappa = 2\gamma$ in Fig. 7, the treatment of decoupling the QD from the cavity is not valid anymore. In these two cases, the numerical results show that

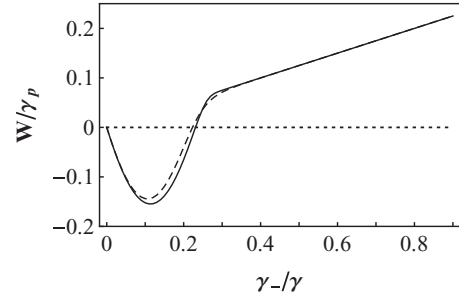


FIG. 8. The quantity W related to the strength of the competitive emission and absorption processes is plotted as a function of γ_- for different values of γ_p with $\bar{n}_p = 5$ in a conventional cavity with decay rate $\kappa = 10^{-3}\gamma$, corresponding to the situation discussed in Fig. 5. $\gamma_p = 10^{-3}\gamma$ (solid line), $10^{-2}\gamma$ (dashed line).

the emission processes govern the absorption processes and the photon number of the cavity is increased.

We recall that, in the case of the low-temperature limit, the statistics of the photon is super-Poissonian for a conventional cavity, Poissonian for a cavity within a PBG material. The presence of the phonon-mediated coupling leads to a reduction of the mean photon number as well as the Mandel's Q parameter as illustrated in Figs. 2–4. This sub-Poissonian character should be attributed to the phonon-mediated coupling. However, a strikingly different effect under the consideration of environmental temperature, i.e., $\bar{n}_p = 5$, is that the total effect of the presence of the phonon-mediated coupling is to increase the values of Mandel's Q parameter regardless of the presence of the PBG material, resulting in a pronounced super-Poissonian statistics [see Figs. 5(b) and 6(b)] or changing from sub-Poissonian statistics to Poissonian statistics [see Fig. 7(b)]. For example, the behavior of the Q parameter is distinct from each other when comparing Figs. 2(b) and 5(b), especially for the case without being engineered in the PBG material. For $\bar{n}_p = 0$, the values of Q parameter are reduced, while for $\bar{n}_p = 5$ they are increased due to the phonon-mediated processes, although both of them correspond to super-Poissonian statistics. The enhanced super-Poissonian statistics and the disappearance of the sub-Poissonian statistics of the off-resonant cavity field lead us to conclude that the phonon-mediated processes arose from the EPI and off-resonant dot-cavity coupling could damage the nonclassical effect of the system when the temperature of the phonon reservoir is considered.

IV. CONCLUSION

We have investigated the influence of the phonon-mediated processes induced by EPI together with the off-resonant dot-cavity coupling on mean photon number and Mandel's Q parameter of the photon field. In the low-temperature limit, the inclusion of the phonon-mediated processes could lead to a reduction of the mean photon number. If $\kappa \ll \gamma$, the threshold behavior is preserved, but the value of Mandel's Q parameter is reduced; if $\kappa = 0.2\gamma$, the photon statistics of the cavity field can be tuned to sub-Poissonian by increasing γ_p . Without being engineered in a PBG material, the interesting nonclassical effect can be achieved due to EPI and the

off-resonant dot-cavity coupling, and the nonclassical effect can be enhanced by the PBG material. When the temperature of the phonon reservoir is considered, i.e., $\bar{n}_p = 5$, the total effect of the phonon-mediated processes is to increase the values of Mandel's Q parameter. The phonon-mediated processes damage the nonclassical effect of the system. If $\kappa \ll \gamma$, the phonon-mediated processes could lead to the increase (decrease) of the photon number when the pumping rate γ_- is smaller (larger) than the effective phonon-mediated threshold γ_-^0 . However, for $\kappa = 0.2\gamma$ or $\kappa = 2\gamma$, the intensity of the cavity photon could be strengthened by phonon-mediated processes arose from the EPI and the off-resonant dot-cavity coupling.

ACKNOWLEDGMENTS

This work is supported by the National Natural Science Foundation of China (Grants No. 11074087 and No. 61275123), and the Nature Science Foundation of Wuhan City (Grant No. 201150530149), and the National Basic Research Program of China (Grant No. 2012CB921602).

APPENDIX: THE EVOLUTION EQUATIONS FOR COMBINATIONS $\rho^{(i)}$

The evolution equations for combinations $\rho^{(i)}$ are obtained from the straightforward calculations for $\dot{\rho}^{(i)}$ according to the

definition (23) with the help of Eq. (22), which are of the form

$$\begin{aligned}\dot{\rho}^{(1)} &= g_1 \rho^{(3)} - g_1 \rho^{(4)} + \kappa \mathcal{L}_c^- \rho^{(1)} + \frac{\gamma_p}{2} \bar{n}_p s^4 \mathcal{L}_p^- (\rho^{(1)} - \rho^{(2)}) \\ &\quad + \frac{\gamma_p}{2} (\bar{n}_p + 1) s^4 \mathcal{L}_c^- (\rho^{(1)} + \rho^{(2)}), \\ \dot{\rho}^{(2)} &= -g_1 \rho^{(3)} + g_1 \rho^{(4)} + \kappa \mathcal{L}_c^- \rho^{(2)} - \gamma_1 \rho^{(1)} - \gamma_{\text{pop}} \rho^{(2)} \\ &\quad - \frac{\gamma_p}{2} (\bar{n}_p + 1) s^4 \mathcal{L}_c^+ (\rho^{(1)} + \rho^{(2)}) \\ &\quad + \frac{\gamma_p}{2} \bar{n}_p s^4 \mathcal{L}_p^+ (\rho^{(1)} - \rho^{(2)}),\end{aligned}\quad (\text{A1})$$

with

$$\begin{aligned}\dot{\rho}^{(3)} &= g_1 \mathcal{L}_p^- \rho^{(1)} + g_1 \mathcal{L}_p^+ \rho^{(2)} + \kappa \mathcal{L}_c^- \rho^{(3)} - \kappa \rho^{(4)} \\ &\quad + \left(\frac{\kappa}{2} - \gamma_{\text{coh}} \right) \rho^{(3)} - \frac{\gamma_p}{2} (\bar{n}_p + 1) s^4 (a^\dagger a - 1) \rho^{(3)} \\ &\quad - \frac{\gamma_p}{2} \bar{n}_p s^4 a a^\dagger \rho^{(3)},\end{aligned}\quad (\text{A2})$$

$$\begin{aligned}\dot{\rho}^{(4)} &= g_1 \mathcal{L}_c^+ \rho^{(2)} - g_1 \mathcal{L}_c^- \rho^{(1)} + \kappa \mathcal{L}_c^- \rho^{(4)} - \left(\frac{\kappa}{2} + \gamma_{\text{coh}} \right) \rho^{(4)} \\ &\quad - \frac{\gamma_p}{2} (\bar{n}_p + 1) s^4 a^\dagger a \rho^{(4)} - \frac{\gamma_p}{2} \bar{n}_p s^4 (a a^\dagger + 1) \rho^{(4)},\end{aligned}$$

with the definition of the operators $\mathcal{L}_{c,p}^\pm \rho^{(i)}$ as

$$\begin{aligned}\mathcal{L}_c^\pm \rho^{(i)} &\equiv (2a \rho^{(i)} a^\dagger \pm a^\dagger a \rho^{(i)} \pm \rho^{(i)} a^\dagger a) / 2, \\ \mathcal{L}_p^\pm \rho^{(i)} &\equiv (2a^\dagger \rho^{(i)} a \pm a a^\dagger \rho^{(i)} \pm \rho^{(i)} a a^\dagger) / 2.\end{aligned}\quad (\text{A3})$$

-
- [1] D. Meschede, H. Walther, and G. Müller, *Phys. Rev. Lett.* **54**, 551 (1985); M. Brune, J. M. Raimond, P. Goy, L. Davidovich, and S. Haroche, *ibid.* **59**, 1899 (1987).
- [2] J. McKeever, A. Boca, A. D. Boozer, J. R. Buck, and H. J. Kimble, *Nature (London)* **425**, 268 (2003); K. An, J. J. Childs, R. R. Dasari, and M. S. Feld, *Phys. Rev. Lett.* **73**, 3375 (1994).
- [3] G. M. Meyer, M. Löffler, and H. Walther, *Phys. Rev. A* **56**, R1099 (1997).
- [4] Z. G. Xie, S. Götzinger, W. Fang, H. Cao, and G. S. Solomon, *Phys. Rev. Lett.* **98**, 117401 (2007).
- [5] M. Nomura, N. Kumagai, S. Iwamoto, Y. Ota, and Y. Arakawa, *Opt. Express* **17**, 15975 (2009).
- [6] T. Pellizzari and H. Ritsch, *Phys. Rev. Lett.* **72**, 3973 (1994).
- [7] J. Wiersig, C. Gies, F. Jahnke, M. Aßmann, T. Berstermann, M. Bayer, C. Kistner, S. Reitzenstein, C. Schneider, S. Höfling, A. Forchel, C. Kruse, J. Kalden, and D. Hommel, *Nature (London)* **460**, 245 (2009).
- [8] R. M. Stevenson, R. J. Young, P. Atkinson, K. Cooper, D. A. Ritchie, and A. J. Shields, *Nature (London)* **439**, 179 (2006); T. M. Stace, G. J. Milburn, and C. H. W. Barnes, *Phys. Rev. B* **67**, 085317 (2003).
- [9] C. Ginzler, H. J. Briegel, U. Martini, B. G. Englert, and A. Schenzle, *Phys. Rev. A* **48**, 732 (1993); M. Löffler, G. M. Meyer, and H. Walther, *ibid.* **55**, 3923 (1997).
- [10] G. X. Li, M. Luo, and Z. Ficek, *Phys. Rev. A* **79**, 053847 (2009).
- [11] R. Wang and S. John, *Phys. Rev. A* **70**, 043805 (2004).
- [12] L. Florescu, S. John, T. Quang, and R. Wang, *Phys. Rev. A* **69**, 013816 (2004); L. Florescu, *ibid.* **78**, 023827 (2008).
- [13] D. Vujic and S. John, *Phys. Rev. A* **76**, 063814 (2007).
- [14] X. Ma and S. John, *Phys. Rev. A* **80**, 063810 (2009); **84**, 053848 (2011).
- [15] P. Gartner, *Phys. Rev. A* **84**, 053804 (2011).
- [16] S. Ya. Kilin and A. B. Mikhalychev, *Phys. Rev. A* **85**, 063817 (2012).
- [17] M. Kaniber, A. Laucht, A. Neumann, J. M. Villas-Boas, M. Bichler, M. C. Amann, and J. J. Finley, *Phys. Rev. B* **77**, 161303(R) (2008).
- [18] O. Painter *et al.*, *Science* **284**, 1819 (1999); S. John, *Phys. Rev. Lett.* **53**, 2169 (1984); **58**, 2486 (1987).
- [19] A. Badolato *et al.*, *Science* **308**, 1158 (2005).
- [20] S. Strauf, K. Hennessy, M. T. Rakher, Y. S. Choi, A. Badolato, L. C. Andreani, E. L. Hu, P. M. Petroff, and D. Bouwmeester, *Phys. Rev. Lett.* **96**, 127404 (2006).
- [21] F. P. Laussy, E. del Valle, and C. Tejedor, *Phys. Rev. Lett.* **101**, 083601 (2008).
- [22] K. Hennessy, A. Badolato, M. Winger, D. Gerace, M. Atatüre, S. Gulde, S. Fält, E. L. Hu, and A. Imamoglu, *Nature (London)* **445**, 896 (2007).
- [23] D. Press, S. Götzinger, S. Reitzenstein, C. Hofmann, A. Löffler, M. Kamp, A. Forchel, and Y. Yamamoto, *Phys. Rev. Lett.* **98**, 117402 (2007).
- [24] U. Hohenester, *Phys. Rev. B* **81**, 155303 (2010).
- [25] A. Majumdar, E. D. Kim, Y. Gong, M. Bajcsy, and J. Vučković, *Phys. Rev. B* **84**, 085309 (2011).
- [26] A. Majumdar, A. Faraon, E. D. Kim, D. Englund, H. Kim, P. Petroff, and J. Vučković, *Phys. Rev. B* **82**, 045306 (2010).

- [27] A. Ulhaq, S. Ates, S. Weiler, S. M. Ulrich, S. Reitzenstein, A. Löffler, S. Höfling, L. Worschech, A. Forchel, and P. Michler, *Phys. Rev. B* **82**, 045307 (2010).
- [28] F. P. Laussy, E. del Valle, and C. Tejedor, *Phys. Rev. B* **79**, 235325 (2009).
- [29] I. Wilson-Rae and A. Imamoglu, *Phys. Rev. B* **65**, 235311 (2002).
- [30] C. Roy and S. Hughes, *Phys. Rev. Lett.* **106**, 247403 (2011).
- [31] C. Roy and S. Hughes, *Phys. Rev. X* **1**, 021009 (2011).
- [32] A. Majumdar, A. Papageorge, E. D. Kim, M. Bajcsy, H. Kim, P. Petroff, and J. Vuckovic, *Phys. Rev. B* **84**, 085310 (2011).
- [33] A. Majumdar, M. Bajcsy, A. Rundquist, E. Kim, and J. Vučković, *Phys. Rev. B* **85**, 195301 (2012).
- [34] A. Majumdar, A. Rundquist, M. Bajcsy, and J. Vučković, *Phys. Rev. B* **86**, 045315 (2012).
- [35] A. Papageorge, A. Majumdar, E. D. Kim, and J. Vučković, *New J. Phys.* **14**, 013028 (2012).
- [36] G. S. Agarwal, L. M. Narducci, D. H. Feng, and R. Gilmore, *Phys. Rev. Lett.* **42**, 1260 (1979).
- [37] M. O. Scully and M. S. Zubairy, *Quantum Optics* (Cambridge University Press, Cambridge, UK, 1997); J. S. Peng and G. X. Li, *Introduction to Modern Quantum Optics* (World Scientific, Singapore, 1998).
- [38] T. Quang and H. Freedhoff, *Phys. Rev. A* **47**, 2285 (1993).
- [39] M. Florescu and S. John, *Phys. Rev. A* **69**, 053810 (2004).
- [40] D. Englund, A. Majumdar, A. Faraon, M. Toishi, N. Stoltz, P. Petroff, and J. Vučković, *Phys. Rev. Lett.* **104**, 073904 (2010).
- [41] A. Rundquist, A. Majumdar, and J. Vučković, *Appl. Phys. Lett.* **99**, 251907 (2011).
- [42] L. Mandel, *Opt. Lett.* **4**, 205 (1979).